

Synthesis and Characterizations of $\text{SiO}_2\text{-Al}_2\text{O}_3$ by Hydrothermal Method

Deepak Tayde^{1*} and Machhindra Lande²

¹ MJM ACS college, Department of Chemistry, Karanjali(Peth), Dist-Nashik, Maharashtra, INDIA

² Department of Chemistry, Dr. Babasaheb Ambedkar Marathwada University, Aurangabad, Maharashtra, INDIA

* Correspondence: E-mail: dtc_chem@yahoo.com

(Received 10 Dec, 2018; Accepted 11 Jan, 2019; Published 18 Jan, 2019)

ABSTRACT: The single metal oxides are having their own specific properties these are mixed together by hydrothermal method to form $\text{SiO}_2\text{-Al}_2\text{O}_3$ mixed metal oxide. This multifunctional mixed metal oxide characterised by analytical instrumental techniques such as XRD, FTIR, SEM-EDS and BET surface area.

Keywords: Metal oxides; Hydrothermal method; Morphology; Particle size.

INTRODUCTION: Metal oxides play a very important role in many areas of chemistry, physics and materials science [1-6]. Metallic elements are able to form a various types of oxide compounds because of their variable oxidation state, reactivity and stability at high temperature. These types of metal oxides having a tendency to adopt vast number of geometrical and electronic structures. These specific structures can exhibit metallic, semiconductor or insulator in character as well as having different active sites those are responsible to enhance chemical reactions [7-11].

Today's technology metal oxides are having huge applications, such as microelectronic circuits, sensors, piezoelectric devices, fuel cells, coatings agent on surfaces against corrosion and as catalysts [12-18]. In the field of solid acid catalyst, the researchers are having goal to prepare nanoparticles, nanorods, nanotubes from metal oxides with special properties.

Nano size metal oxides and mixed metal oxides can exhibit unique physical and chemical properties due to their limited size and a high density of corner or edgesurface sites [19-23]. Any particle size is having own identity because of its three important basic properties. The properties are structural characteristics, lattice symmetry and cell parameters. These three properties are just like DNA code of our metal oxide material. Large size metal oxides are usually strong and stable systems with well-defined crystallographic structures [24-28]. Because of the change in thermodynamic stability the particle size of metal oxides decreases with increases in surface free energy and stress [29-34].

MATERIALS AND METHODS:

Synthesis of $\text{SiO}_2\text{-Al}_2\text{O}_3$ Mixed Metal Oxides by Hydrothermal Method: The SiO_2 and $\text{SiO}_2\text{-Al}_2\text{O}_3$ metal oxide and mixed metal oxides were prepared by hydrothermal method. In a typical synthesis, 1gm cetyl trimethyl ammonium bromide (CTAB) was added in mixture of 8.33mL of tetraethyl ortho silicate (TEOS), aqueous solution of 0.25 gm of aluminum nitrate ($\text{Al}(\text{NO}_3)_3$). Add 5 mL 1:1 aqueous sodium hydroxide (aq. NaOH) to maintain PH up to 9-10 and stirred this mixture at room temperature for 24 h to obtained precipitate. Then this mixture of precipitate hydrothermally treated at 150°C for 5 h in high pressure autoclave at 400 rpm having autogeneous pressure 54 psi at the volume 250 mL of mixture. After this mixture was cooled at room temperature solid material obtained was filtered and washed with deionised water, dried at 80°C for 6 h and calcined at 500°C for 3 h. This procedure is repeated for synthesis of SiO_2 metal oxide. The systematic preparation of metal oxide and mixed metal oxides are shown in Fig.1.

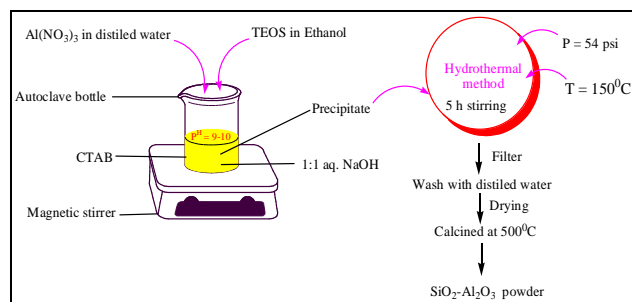


Figure 1: Synthesis of $\text{SiO}_2\text{-Al}_2\text{O}_3$ mixed metal oxide by hydrothermal method.

To study effect of ammonium chloride on acidic properties of catalyst. Take 10 gm SiO₂-Al₂O₃ mixed metal oxide powder was taken in the 250 mL beaker, the aqueous solution of 50 mL ammonium chloride was added with constant stirring; up to 5 h. Then the solution was filtered, dried and calcined at 500°C in the muffle furnace.

RESULTS AND DISCUSSION:

Characterization of SiO₂ and SiO₂-Al₂O₃:

X-Ray Diffraction Study (XRD): The XRD pattern was used to determine geometry and crystallinity of synthesised material. The powder X-ray diffraction pattern of SiO₂ shows a broad peak indicate the amorphous nature of silicon dioxide shown in Fig.2. The XRD pattern of synthesised SiO₂-Al₂O₃ is shown in Fig.3. It shows the orthorhombic crystal structure which is matched with JCPDS card no 84-1566 having parameters a=7.503, b=7.738, c=5.804. Here (111) plane with broad peak indicate that the amorphous nature of SiO₂-Al₂O₃ catalyst. JCPDS card number confirms the siliminite type of zeolite material. Fig.4 show the XRD pattern of NH₄Cl treated siliminite type zeolite, crystallinity decreases after NH₄Cl treatment.

X-ray powder diffraction pattern analysis data of SiO₂ sample exhibits the formation of hexagonal solid solution, the broad peaks were obtained at 2θ = 21.74° corresponding to the planes (100) indicates the hexagonal structure of SiO₂ (Table 1). Al₂O₃ is incorporated into SiO₂ to form SiO₂-Al₂O₃ binary metal oxide. This SiO₂-Al₂O₃ show orthorhombic phase and broad peaks was obtained at 11.83°, 21.64° and 26.45° corresponding to the planes 100, 111 and 210 respectively (Table 2).

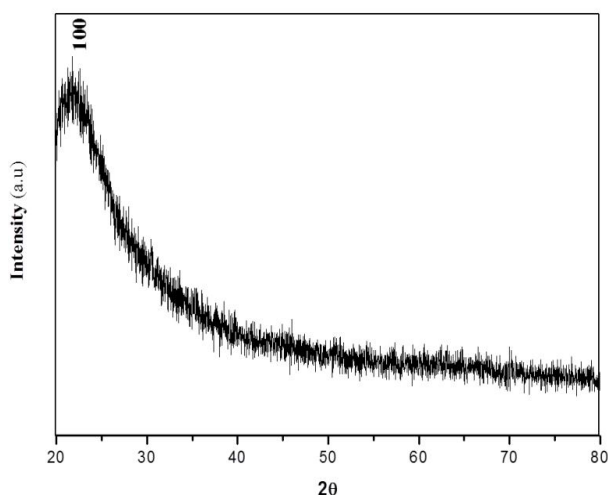


Figure 2: XRD pattern of SiO₂.

Table 1: XRD analysis data of SiO₂.

hkl	2θ (Exp.)	2θ (Calc.)	d (Exp.)	d (Calc.)	Intensity (Exp.)
100	21.746	21.799	4.0836	4.0737	1800.21
002	33.659	34.055	2.6605	2.6305	733.84
110	38.506	38.235	2.3360	2.3520	599.65
111	42.494	42.047	2.1256	2.1471	521.02
201	47.672	47.849	1.9061	1.8994	453.53
103	57.021	57.139	1.6138	1.6107	404.52
210	59.615	60.037	1.5496	1.5397	384.96
210	60.106	60.037	1.5381	1.5397	391.66
211	62.451	62.834	1.4858	1.4777	402.71
211	63.104	62.834	1.4720	1.4777	394.26
113	66.302	66.447	1.4086	1.4058	379.55
300	69.350	69.119	1.3539	1.3579	336.78
203	70.750	70.847	1.3305	1.3289	343.19
004	71.322	71.700	1.3213	1.3152	344.55
104	75.64	75.967	1.2562	1.2516	318.01
302	79.225	79.343	1.2081	1.2066	317.31

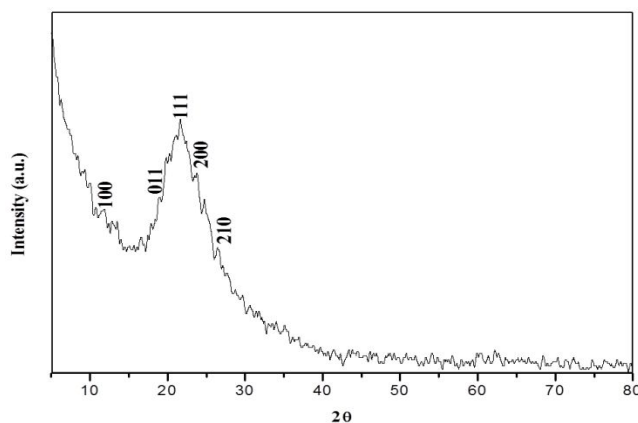


Figure 3: XRD pattern of SiO₂-Al₂O₃.

Table 2: XRD analysis data of SiO₂-Al₂O₃.

hkl	2θ (Exp.)	2θ (Calc.)	d (Exp.)	d (Calc.)	Intensity (Exp.)
101	11.835	11.785	7.4718	7.5030	102.88
011	18.913	19.099	4.6885	4.6430	108.78
111	21.647	22.501	4.1020	3.9482	147.35
200	23.824	23.698	3.7318	3.7515	120.37
210	26.455	26.381	3.3663	3.3757	83.28

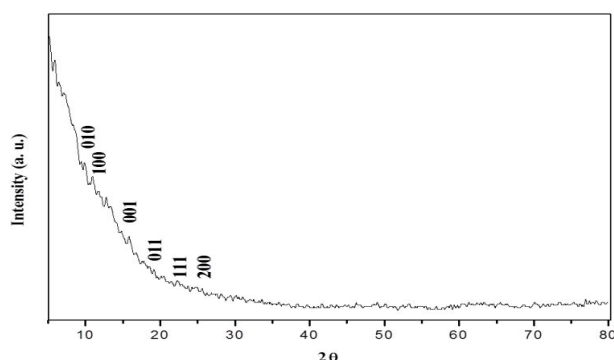


Figure 4: XRD pattern of ammonium chloride treated SiO₂-Al₂O₃.

Table 3: XRD analysis data of SiO₂-Al₂O₃.

hkl	2θ (Exp.)	2θ (Cal.)	d (Exp.)	d (Cal.)	Intensity (Exp.)
010	10.931	11.426	8.0873	7.7380	105.74
100	11.698	11.785	7.5586	7.5030	94.93
001	15.804	15.253	5.6029	5.8040	61.63
011	18.577	19.099	4.7724	4.6430	39.59
111	22.298	22.501	3.9838	3.9482	29.24
200	23.703	23.698	3.7507	3.7515	25.33

Estimation of Crystallite Size Using Debye-Scherrer Equation: The average size (T) of different ratio SiO₂-Al₂O₃ solid materials can be estimated from X-ray line broadening using the Debye-Scherrer equation.

$$T = \frac{0.94\lambda}{\beta \cos \theta}$$

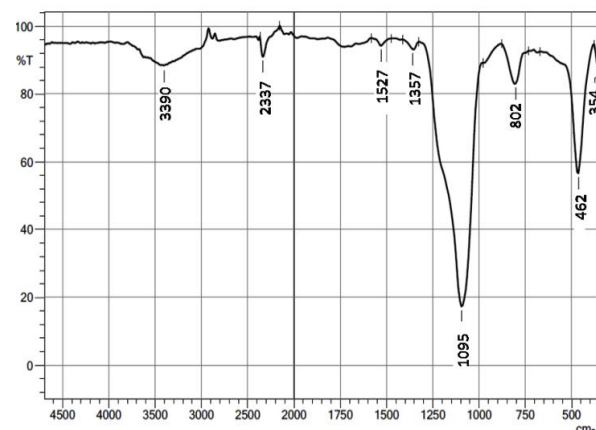
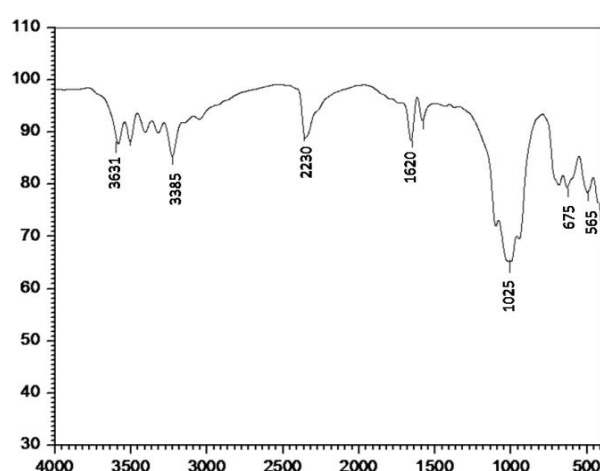
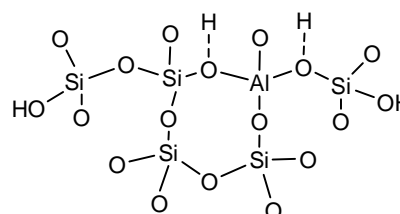
Where, T = average particle size,
 λ = wavelength,
 θ = diffraction angle,
 β = FWHM (Full width half maximum).

The average crystallite sizes of the powder were calculated using Debye-Scherrer formula and listed in Table 4, showing the grain size of SiO₂, SiO₂-Al₂O₃ and NH₄Cl treated SiO₂-Al₂O₃ in the range of 10 - 16 nm. It shows gradual increases in grain size after NH₄Cl treatment on SiO₂-Al₂O₃ catalyst.

Table 4: The average crystallite size calculated by Debye-Scherrer formula.

Entry	Metal Oxides	2θ	FWHM	Crystallite Size (nm)
1	SiO ₂	21.74	0.7287	11
2	Calcined SiO ₂ -Al ₂ O ₃	21.66	0.7500	10
3	NH ₄ Cl treated SiO ₂ -Al ₂ O ₃	10.93	0.4800	16

FTIR Analysis: Fig.5 shows the FT-IR spectrum of the synthesized SiO₂ material. The absorption band at 3390 cm⁻¹ for Si-OH bridged, 2337 cm⁻¹ is like SiO₂ glass, 1527 cm⁻¹ for Si-O stretching vibration and 1095, 802, 462, 354 cm⁻¹ due to the Si-O-Si bending vibration mode. Fig.6 shows the FT-IR spectra of the SiO₂-Al₂O₃ materials having absorption band at 3631 and 3385 cm⁻¹ assign as terminal and bridged Si-OH stretching vibration respectively, 2230 cm⁻¹ band assign as SiO₂ glass, 1620 cm⁻¹ due to the Si-OH bending mode, 1025 cm⁻¹ for Al-OH symmetric bending and 675, 565 cm⁻¹ due to the Si-O-Al bending vibration mode [35-36].

**Figure 5: FTIR spectrum of SiO₂.****Figure 6: FTIR spectrum of SiO₂-Al₂O₃.****[Plausible structure of SiO₂-Al₂O₃ catalyst]**

From the above FTIR data of metal oxide SiO₂ and mixed metal oxide SiO₂-Al₂O₃ are used to predict the plausible structure by referencing their IR frequency. The oxidation state of the metals in the prepared SiO₂-Al₂O₃ catalyst is Al (III) and Si (IV).

SEM-EDS Analysis: Surface morphology of the prepared SiO₂-Al₂O₃ by hydrothermal method was studied by SEM image. In the Fig.7 (a) shows the flakes like structure of SiO₂ oxide. When the Al₂O₃ is doped on the surface of SiO₂ which is observed on the surface in the form of white spots with porous nature in Fig. 7 (b).

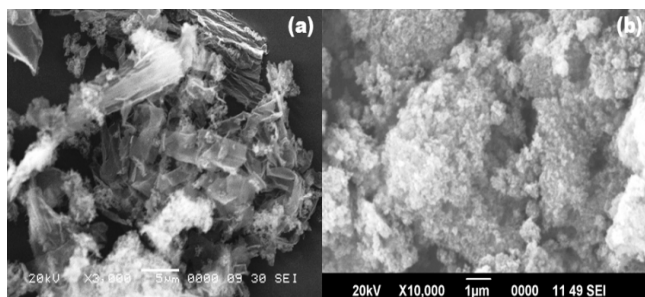


Figure 7: SEM image of a) SiO₂ b) SiO₂-Al₂O₃ calcined at 500^oC.

EDS Spectrum of SiO₂-Al₂O₃: Elemental composition of SiO₂-Al₂O₃ catalysts is represented in Fig.8. The intense peaks in the figure show the presence of Si, Al and O. Elemental composition of SiO₂-Al₂O₃ is mention in Table 2.3.5. The minimum stoichiometric ratio was maintained.

Table 5: EDS elemental quantitative analysis of SiO₂-Al₂O₃.

Constituents	Mass (%)	Atom (%)
Si	57.91	44.41
Al	1.94	1.55
O	40.15	54.05
Total	100.00	100.01

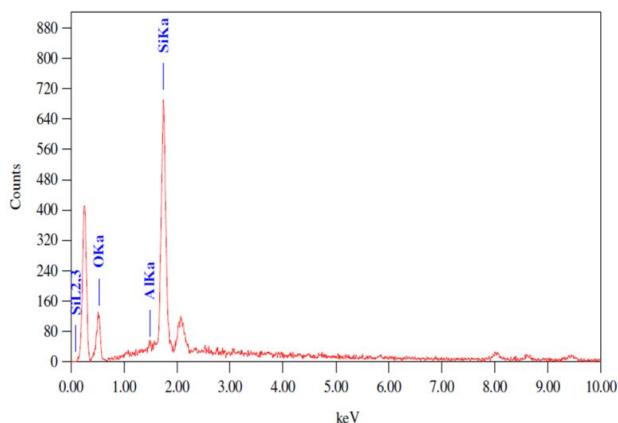


Figure 8: EDS spectrum of SiO₂-Al₂O₃.

BET Surface Area Analysis: BET analysis provides specific surface area evaluation of materials by nitrogen multilayer adsorption measured as a function of relative pressure using a fully automated analyzer. The technique bound external area and pore area evaluations to determine the total specific surface area in m²/g yielding important information in studying the effects of surface porosity and particle size in many applications. From the textural properties of SiO₂-Al₂O₃ the specific surface area 80.3224 m²/g of SiO₂-Al₂O₃ was calculated from BET measurements (Fig. 9) and BJH adsorption average pore diameter is 27.3950 nm (Fig. 10).

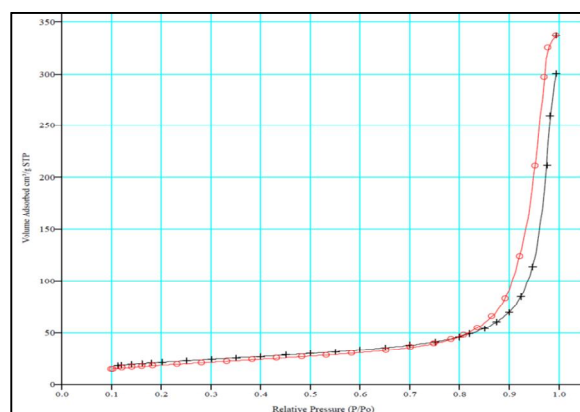


Figure 9: N₂ adsorption/desorption isotherm of SiO₂-Al₂O₃.

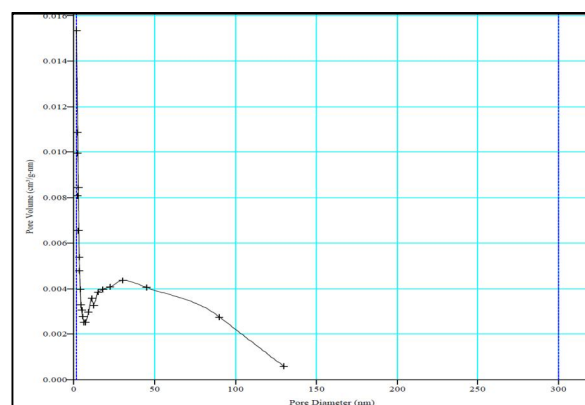


Figure 10: BJH adsorption cumulative pore diameter SiO₂-Al₂O₃.

CONCLUSION: We analyze the internal structure, external morphology, particle size and chemical bonding characterized by XRD, SEM- EDS and FTIR analytical instrumental techniques.

ACKNOWLEDGEMENT: We are grateful to the Head, Department of Chemistry, Dr. B.A.M. University, Aurangabad, 431004 (MS), India and Principal of MJM ACS college for providing the laboratory facility. The author DTT is thankful to UGC New Delhi for providing JRF for financial support. The authors are also thankful to STIC Cochin for characterization facilities.

REFERENCES:

1. Rao M. C., Ravindranadh K., Ramesh K. K. D., Srikanth K. S. (2016) *Der. Pharma. Chemica.*, 8(7), 74.
2. Aggarwal S., Ramesh R. (1998) *Annual Rev. Mater. Sci.*, 28, 463.
3. Stengl V., Henych J., Janos P., Skoumal M. (2016) *Rev. Environ. Contam. Toxicol.*, 58, 236.
4. Hoang K., Johannes M. (2016) *Chem. Mater.*, 28 (5), 1325.

5. Liu S., Liu Q., Smith S., Boerio-Goates J., Woodfield B. (2007) *N.S.T.I. Nanotech.*, 4, 214.
6. Wua Z. S., Zhoua G., Yina L. C., Rena W., Lia F., Cheng H. M. (2012) *Nano Energy.*, 1, 107.
7. Srivastava S., Kumar M., Agrawal A., S. Dwivedi K. (2013) *J. Appl. Phys.*, 5(4), 61.
8. K. Ravindranadh, B. Radhakrishna, M. C. Rao, (2016). *J. Chem. Pharma. Res.*, 8(5), 721.
9. Garcia M. F., Rodriguez J. A. (2007) *Nanomater: Inorg. Bioinorg. Perspectives.*, 1.
10. Strassler S., Reis A., (1983) *Sensors Actuators.*, 4, 465.
11. Kannan S., (2013) *Barc Newsletter*, 331, 1.
12. Warren J., (1998) *Semiconductor Inter.*, 111.
13. Fine G. F., Cavanagh L. M., Afonja A., Binions R., (2010). *Sensors* 10, 5469.
14. Dahiya R. S., Metta G., Valle M., Adami A., Lorenzelli L., (2009) *Appl. Phys. Lett.* 95 (034105), 1.
15. Zuo C., Liu M., Liu M. (2012) *Adva. Sol-Gel Derived Mater. Technol.*, 7.
16. Popoola A., Olorunniwo O. E., Ige O. O. (2014) *Intect. Open Sci.Open Mind.*, 241.
17. Mohapatra M., Anand S. (2010) *Int. J. Eng. Sci. Technol.*, 2(8), 127.
18. Keav S., Matam S. K., Ferri D., Weidenkaff A. (2014) *Catalysts.*, 4, 226.
19. Rao M. C., Ravindranadh K., (2013). *I.J.A.P.B.C.*, 2(1), 225.
20. Raghavendra S., Jayashree P. (2015) *2nd Int. Conference on Sci.,Tecnol. Manag.*, 2846.
21. Sabourimanesh A., Rashidi A., Marjani K., Motamedara P., Valizadeh Y. (2015) *Cryst. Stru. Theory Appl.*, 4, 28.
22. Huang B., Cao M., Nie F., Huang H., Hu C., (2013). *Defence Technol.*, 9, 59.
23. Hussien N. H., Sheltawy S., Abd H. E., Diwani G. E., Shaarawy H. H. (2014) *R.J.P.B.C.S.*, 5(4), 166.
24. Phanichphant S. (2014) *Procedia Eng.*, 87, 795.
25. Zamiri R., H. Ahangar A., Kaushal A., Zakaria A., Zamiri G., Tobaldi D., J. M. F. Ferreira, (2015). *PLOS ONE.*, 10(4), 1.
26. Rao C. N. R. (1989) *Annu. Rev. Phys. Chem.*, 40, 291.
27. Paez A. M. (1994) *J. Chem. Educ.*, 71 (5), 381.
28. Freund H. J. (1995) *Phys. stat. sol. (b)*, 192, 407.
29. Tamaekong N., Liewhiran C., Phanichphant S.,(2014) *J. Nanomater.*, 1.
30. Runge K. C., Tabosa E., Jankovic A., (2013). *2nd Ausimm Inter. Geometallurgy Conf.*, 335.
31. Li W., Ni C., Lin H., Huang C. P., Ismat Shah S., (2004). *J. Appl. Phys.*, 96 (11), 6663.
32. Gribb A. A., Banfield J. F. (1997) *American Mineralogist.*, 82, 717.
33. Kor M., Abkhoshk E., Gharibie K., Shafaei S. Z., (2010) *Int. J. Mining environmental issue.*, 1(1),41.
34. Zhang B., Edwards B. J., (2015) *J. Chem. Phys.*, 142 (214907), 1.
35. Ghamari M., Ghasemifard M. (2017) *J. Korean Ceramic Soc.*, 54 (2), 102.
36. Acchar W., Bezerra da Silva J. R. (2006) *Mater. Res.*, 9(3), 271.